

# Predicting Viruses Accurately by a Multiplex Microfluidic Loop-Mediated Isothermal Amplification Chip

Xueen Fang,<sup>†,‡</sup> Hui Chen,<sup>†</sup> Shaoning Yu,<sup>†</sup> Xingyu Jiang,<sup>\*,‡</sup> and Jilie Kong<sup>\*,†</sup>

<sup>†</sup>Department of Chemistry and Institutes of Biomedical Sciences, Fudan University, Shanghai 200433, P.R. China

<sup>‡</sup>CAS Key Lab for Biological Effects of Nanomaterials and Nanosafety, National Center for Nanoscience and Technology, Beijing 100190, P.R. China

 Supporting Information

**ABSTRACT:** Multiplex gene assay is a valuable molecular tool not only in academic science but also in clinical diagnostics. Multiplex PCR assays, DNA microarrays, and various nanotechnology-based methods are examples of major techniques developed for analyzing multiple genes; none of these, however, are suitable for point-of-care diagnostics, especially in resource-limited settings. In this report, we describe an octopus-like multiplex microfluidic loop-mediated isothermal amplification ( $m\mu$ LAMP) assay for the rapid analysis of multiple genes in the point-of-care format and provide a robust approach for predicting viruses. This assay with the ability of analyzing multiple genes qualitatively and quantitatively is highly specific, operationally simple, and cost/time-effective with the detection limit of less than 10 copies/ $\mu$ L in 2  $\mu$ L quantities of sample within 0.5 h. We successfully developed a  $m\mu$ LAMP chip for differentiating three human influenza A substrains and identifying eight important swine viruses.

The epidemic of severe acute respiratory syndrome in 2003,<sup>1</sup> highly pathogenic avian flu in 2005,<sup>2</sup> and swine-origin pandemic influenza A H1N1 in 2009<sup>3,4</sup> showed the formidable force of viruses in the front of the human being. The variability speed of the virus exceeds our imagination. It is expected that we will be possibly confronted with more powerful viruses in the future. Effective approaches to the differentiation and identification of these viruses is therefore critical for the surveillance, control, and therapeutics of an epidemic.

The multiplex gene assay is a powerful molecular tool for analyzing viruses in clinical diagnostics.<sup>5</sup> Three major techniques were developed to analyze multiple genes, namely, multiplex PCR assays,<sup>6,7</sup> DNA microarrays,<sup>8–10</sup> and nanotechnology-based methods.<sup>11–13</sup> Multiplex PCR was one of the most typical methods for analyzing multiple genes. However, this method was limited to the analysis of only some targets because of the incompatibility of different primer sets in the same reaction system.<sup>14</sup> DNA microarray technique has the capability to analyze ultrahigh throughput targets in parallel but is still limited in the application of rapid clinical diagnostics because it takes a long time and is costly. Nanotechnology-based nucleic acid sensors have experienced rapid development in recent years, but many of them are still not practical in real applications. In addition, most of these methods demand sophisticated instruments, well-equipped laboratories, and specially trained technicians, which are not suitable for point-of-care applications, especially in resource-limited settings.

It is really a miracle that the famous Octopus Paul accurately predicted the results of the World Cup 2010 in South Africa. It would be more exciting if Paul can accurately predict viruses in diagnostics. Here we integrate the merits of loop-mediated isothermal amplification (LAMP)<sup>15,16</sup> and microfluidics<sup>17–19</sup> to develop an octopus-like inexpensive portable device, termed as multiplex microfluidic LAMP ( $m\mu$ LAMP) for the rapid analysis of multiple genes and point-of-care virus diagnostics.

In this report, we first presented a  $m\mu$ LAMP system for differentiating three influenza A subtypes, including influenza A virus (flu A), seasonal influenza A H1N1 virus (seasonal H1N1), and 2009 pandemic influenza A H1N1 virus (pandemic H1N1). Successfully screening effective biomarkers with low cross reactivity and high reliability would be the first step to establishing such a  $m\mu$ LAMP system.<sup>20</sup> Therefore, we determined three conserved gene fragments as specific biomarkers for these subtypes of influenza A virus. First, we obtained nucleic acid sequences for 1500 isolates/strains of influenza A subtypes from American GeneBank. After analyzing by Vector NTI, the conserved fragments of the matrix gene (Accession Number FJ520167; DNA fragment, 131–303) and hemagglutinin gene (Accession Number, CY054553; DNA fragment, 970–1169; Accession Number, AB514226; DNA fragment, 765–956) were chosen as the molecular biomarker to identify flu A, seasonal H1N1, and pandemic H1N1, respectively. The detailed sequences of these gene fragments are in the Supporting Information, Table S1. We used the BLAST program to confirm the conservation of these gene biomarkers (Supporting Information, Figure S1). Successfully designing specific probes to recognize these biomarkers is a vital aspect for developing this novel bioassay. We used Primer Explorer V3 software (<http://primerexplorer.jp/e/>) to design the corresponding probe sets. Each set included six probes, namely, F3/B3, FIP/BIP, and LF/LB. LAMP amplification will proceed and a positive signal generated only if all of the probes interact with the gene biomarker.<sup>15</sup> Detailed probe set sequences are in the Supporting Information, Table S2. Apart from the conserved gene marker and its corresponding specific probe sets, we established optimized  $m\mu$ LAMP reaction conditions by screening the suitable concentration of  $Mg^{2+}$ , dNTPs, probes, and temperature using agarose gel electrophoresis to provide the best microenvironment for

**Received:** November 1, 2010

**Accepted:** December 3, 2010

**Published:** December 10, 2010

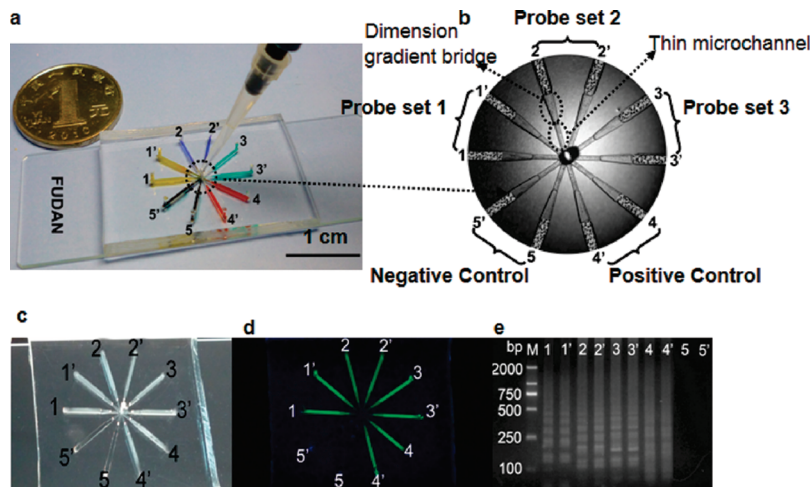


**Figure 1.**  $m\mu$ LAMP for the point-of-care analysis of multiple genes. (a) Photograph of the 10 microchamber  $m\mu$ LAMP system in a PDMS-glass format. (b) Structure of the  $m\mu$ LAMP chip. Microchambers (length, 7 mm; width, 0.6 mm; depth, 0.8 mm) were connected to the corresponding thin microchannel (length, 2 mm; width, 0.2 mm; depth, 0.2 mm) via dimension gradient bridges (length, 2 mm; width, 0.2 → 0.6 mm; depth, 0.5 mm) with the whole shape like an octopus. Microchamber 1/1', 2/2', and 3/3' were coated with seasonal H1N1-probes, flu A-probes, and pandemic H1N1-probes, respectively; The fourth microchamber set (4 and 4') loaded with human  $\beta$  actin-probes was applied as a positive control while the chamber 5/5' with no probes patterned worked as the negative control. (c) Direct naked-eye determination of the assay result via the insoluble byproduct magnesium pyrophosphate. Microchamber 1/1', 2/2', 3/3', and 4/4' were positive with white turbidity, whereas chambers 5/5' displayed negative results. (d) These results were further validated by the green fluorescence induced by the DNA-intercalating dye SYBR green I and (e) the characteristic ladderlike pattern of the LAMP product determined by agarose gel electrophoresis.

the specific probes to effectively recognize the gene markers of influenza A subtypes and trigger the positive visible signal of turbidity (Supporting Information, Figure S2). After establishing the bioreaction for the detection of each influenza A virus gene marker, we created an octopus-like microfluidic chip to simultaneously analyze these gene markers in one setting.

This microfluidic chip was designed to have 10 microchambers and each was connected to the corresponding thin microchannel via a dimension gradient bridge (Figure 1a,b). This structure was critical for the performance of  $m\mu$ LAMP. Thin microchannels with low-mass-transfer coefficients were designed to forbid the cross-talk of probes among different microchambers, while dimension gradient bridges (the dimension of the bridge changes gradually) work as a connector between the thin microchannel and the microchamber, making the loading of reaction buffer more smooth. In addition, this configuration of microfluidic chip would not affect the LAMP performance when compared to typical reaction tubes. All of microchambers were precoated with certain quantities of specific LAMP probe sets using the flow patterning technique. Microchamber 1/1', 2/2', and 3/3' were coated with seasonal H1N1-probes, flu A-probes, and pandemic H1N1-probes, respectively. These functionalized microchannels could recognize the specific nucleic acid fragment of influenza A subtypes in situ, permitting the rapid amplification and simultaneously triggering the LAMP signal. We also functionalized the fourth set of microchambers (4/4') with human  $\beta$  actin-probes as positive controls, whereas 5/5' contained no probes as negative controls. These two sets of microchambers assessed the efficiency of the assay and made the final results much more reliable and convincing. In all experiments, we allowed each probe set to perform the target recognition twice in order to enhance the reproducibility of the system and provide more stable test results. Both the sample and LAMP reaction buffer were subsequently introduced at the central hole, filling all 10 microchambers by capillary force. We created the integral chip

by applying uncured polydimethylsiloxane (PDMS), tightly sealing at the inlet/outlet, and incubated the chip at 63 °C for 1 h to complete the test. The final result was directly determined by the naked eye based on the white precipitate of magnesium pyrophosphate generated in the reaction.<sup>21</sup> The results were further confirmed by SYBR green I fluorescence and standard agarose gel electrophoresis (Figure 1c–e).

We evaluated the ability of the device by measuring standards of influenza A subtypes. We observed that each standard only triggered the LAMP signal in its corresponding microchamber and no cross-activity appeared in this setup (Figure 2a–c, a'–c'). The probe set and white precipitate in its corresponding microchamber would not mix with those in adjacent chambers. This phenomenon was critical to the performance of  $m\mu$ LAMP, permitting the spatial differentiation of signal and providing the possibility of simultaneously analyzing multiple targets in one system.

To further validate the performance of the chip, we applied reference strains. Seasonal H1N1 triggered the signal in chamber 1/1', 2/2', and 4/4'. Pandemic H1N1 triggered a positive signal in chamber of 2/2', 3/3', and 4/4', while flu A triggered the signal in chamber 2/2' and 4/4'. None of these samples could induce the white precipitate in the negative control chamber (Figure 2e–g, e'–g'). The occurrence of turbidity in microchamber 2/2' in the presence of the seasonal or pandemic H1N1 demonstrated that both of the viruses belong to the classification of the flu A. The successful extraction of target nucleic acids from the human-related specimens induced a positive response of microchamber 4/4' due to the presence of the human  $\beta$  actin gene fragment in the sample. The different patterns of the  $m\mu$ LAMP signal presented here permitted the differentiation of influenza A subtypes and identification of the 2009 pandemic influenza A (H1N1) virus effectively.

We applied this  $m\mu$ LAMP chip to the analysis of two nonhuman viruses, swine H1N1 and H2N3. Both of the virus induced the signal of white turbidity or green fluorescence in the microchamber 2/2' (Figure 2d,d',h,h'), implying that these two

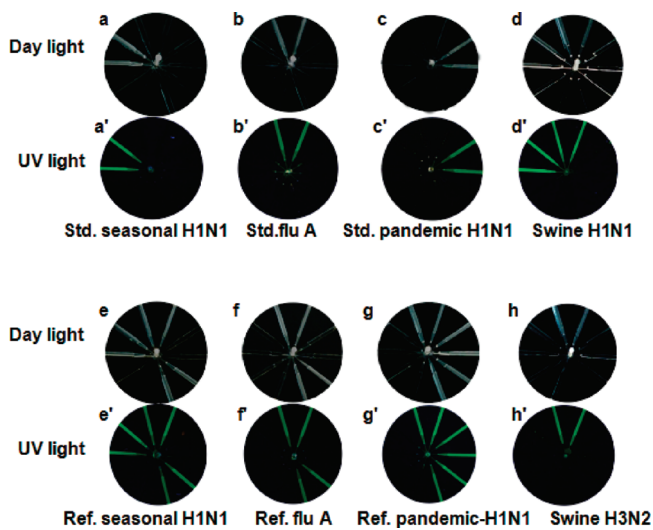


**Figure 2.** Performance of  $m\mu$ LAMP for analyzing three influenza A subtypes. (a–h) Signal pattern of white turbidity formed by the precipitate of magnesium pyrophosphate and (a'–h') green fluorescence induced by the DNA intercalating dye SYBR green I for the standard sample of seasonal H1N1 (a, a'), flu A (b, b'), and pandemic H1N1 (c, c'); reference strains of seasonal H1N1 (e, e'), flu A (f, f'), and pandemic H1N1 (g, g'); two other nonhuman viruses, swine H1N1 (d, d') and H3N2 (h, h').

species belong to the same category as the flu A virus in the terms of evolutionary relationship. We also observed that swine H1N1 caused a positive signal in the microchamber 1/1', revealing the closer genetic relationship with the common human seasonal H1N1 than pandemic H1N1. Thus, we think our assay has potential for analyzing the origin or genetic relationship of living species.

Our novel device was further validated using clinical samples and compared to the standard PCR method. Clinical samples 1–4 were confirmed to be the pandemic H1N1 according to the similar signal pattern as that obtained with the reference, which correlated well with the result from the PCR assay (Table 1). Samples 5 and 6 simultaneously induced positive signals in microchambers 1/1', 2/2', 3/3', and 4/4'. We attributed this phenomenon to the following: the pandemic H1N1 varied or the sample was contaminated by both seasonal H1N1 and pandemic H1N1. Because of a lack of positive signal in the chamber 2/2', samples 7 and 8 were determined not to be the flu A species. These two samples were identified as the influenza B virus using PCR by the Shanghai Public Health Clinical Center. Because of high-speed variability of the influenza A virus, screening suitable LAMP probes would be critical to avoid false positive/negative test results.

To further show that our device can be easily expanded for quantitative assays, we demonstrated real-time quantitative  $m\mu$ LAMP by measuring the time-to-positive (TTP) value of the reaction. Many studies have shown that the TTP value of LAMP correlates with the original concentration of the target.<sup>22,23</sup> We previously applied a transmissible light-based optical sensor to monitor the TTP value in the microchamber.<sup>22</sup> To make the device more compact, we used a different optical format based on the reflected optical fiber (Figure 3a). In this format, the emission light from the fiber first traverses the LAMP reaction chamber, then reflected by a mirror underneath the chip,

**Table 1. Detail Results of the  $m\mu$ LAMP for Analyzing Influenza A Subtypes and Clinical Specimens<sup>a</sup>**

sample name	1/1'	2/2'	3/3'	4/4'	5/5'
standard sample of seasonal H1N1	+	–	–	–	–
standard sample of flu A	–	+	–	–	–
standard sample of pandemic H1N1	–	–	+	–	–
reference strain of human seasonal H1N1	+	+	–	+	–
reference strain of human flu A	–	+	–	+	–
reference strain of human pandemic H1N1	–	+	+	+	–
reference strain of swine H1N1	+	+	–	–	–
reference strain of swine H2N3	–	+	–	–	–
clinical sample 1	–	+	+	+	–
clinical sample 2	–	+	+	+	–
clinical sample 3	–	+	+	+	–
clinical sample 4	–	+	+	+	–
clinical sample 5	+	+	+	+	–
clinical sample 6	+	+	+	+	–
clinical sample 7	–	–	–	+	–
clinical sample 8	–	–	–	+	–

<sup>a</sup> “+” denotes the positive signal while “–” refers to the negative signal.

and finally recorded by the digital sensor. The generation of white precipitate in the microchamber could decrease the intensity of both the emitted and reflected light, which could be recorded by this optical sensor in real time.

We applied this system to obtain the dynamic curve of each standard using 10-fold serial dilutions with the concentration ranging from  $10^2$  to  $10^6$  fg/ $\mu$ L, and the corresponding TTP values were recorded simultaneously. The standard curves were established by plotting the TTP value versus log concentration of standards for the quantitative analysis. We obtained standard curves with correlation coefficients of 0.9984, 0.9897, and 0.9962 for flu A, seasonal H1N1, and pandemic H1N1, respectively (Figure 3b). Although the fluctuation of the dynamic curve could not be totally avoided between runs using this homemade device, the TTP values of standard dilutions were much more stable, which insures the accuracy of the quantitative results. This device with the ability of determining the quantities of the target could be extremely useful for point-of-care quantitative gene analysis and the determination of the quantity of pathogens in clinical diagnostics, especially in resource-limited areas.

Next, we investigated the sensitivity, specificity, and speeding of this novel  $m\mu$ LAMP. We used 10-fold serial dilutions of standards to evaluate the sensitivity of the assay. It exhibited high sensitivity with a detection limit of 9 copies/ $\mu$ L, 10 copies/ $\mu$ L, and 8 copies/ $\mu$ L for flu A virus, seasonal H1N1, and pandemic H1N1 subtypes, respectively (Figure 4a). The sensitivity of this  $m\mu$ LAMP for the pandemic H1N1 was also verified to be 100–1000-fold higher than that of the standard PCR (Supporting Information, Figure S3). This detection limit of this assay appears to exceed that of most other methods and could be compared with real-time PCR assays.<sup>24,25</sup> We believe this novel assay could meet the requirement of most of the diagnostics for various pathogens or genetic diseases.

To investigate the specificity, we used the blank PUC57 plasmid as the template to test the assay. None of the functional microchambers recognized the blank plasmid (Figure 4b, lane 10). After insertion of the target gene fragment into PUC57, the corresponding chamber triggered the LAMP signal and the

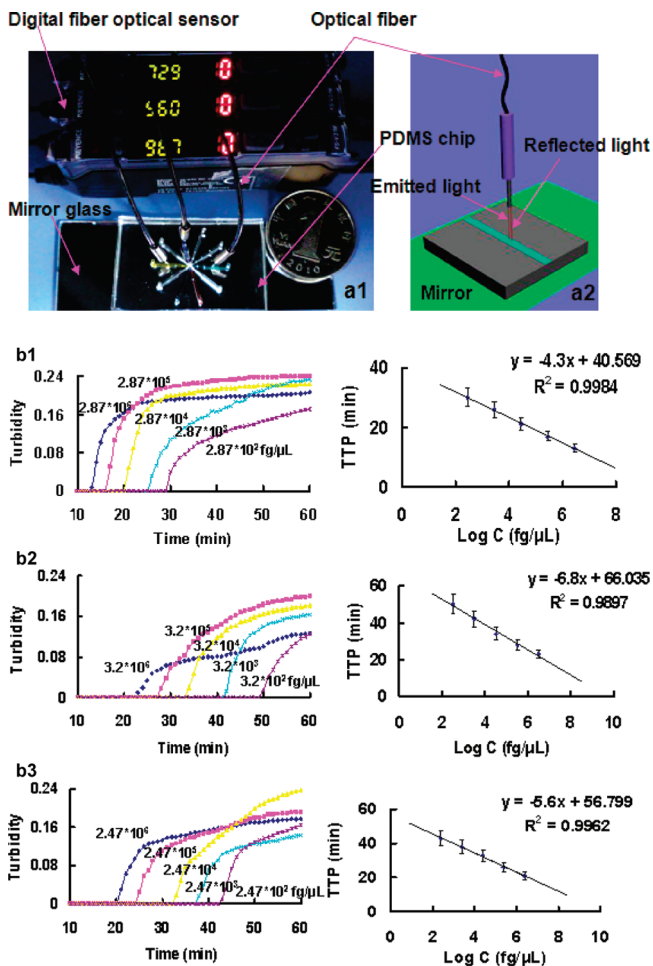


**Figure 3.** Quantitative mμLAMP based on the reflected optical sensor. (a) Photograph (a1) and schematic diagram (a2) of the quantitative mμLAMP setup. (b) Dynamic (left) and standard curves (right) of the flu A (b1), seasonal H1N1 (b2), and pandemic H1N1 (b3).

ladderlike pattern in gel electrophoresis (Figure 4b, lane 1). To evaluate the specificity of this system, we also attempted to use other viruses, including foot-and-mouth disease virus (FMDV), porcine reproductive and respiratory syndrome virus (PRRSV), classical swine fever virus (CSFV), transmissible gastroenteritis of swine virus (TGEV), and pseudo rabies virus (PRV) for testing. No LAMP bands were observed in gel electrophoresis, demonstrating that this mμLAMP was specific to the target virus and did not have cross-talk with other viruses. The specificity of LAMP reaction products was further confirmed by the expected digestion bands in gel electrophoresis when analyzed by *Pst* I, *Bam* AI (Figure 4b, lane 2). This high selectivity of the system was ensured by the specific LAMP probes binding simultaneously with the six distinct sequences of the gene marker.<sup>15</sup> The fast response time was another virtue of the mμLAMP system. We found that 5 min was enough to trigger the LAMP signal for microchamber 2, 10 min for chamber 3, and 20 min for chamber 1, which was relatively fast when compared with other nucleic amplification-based analytical methods (Figure 4c).

Many previously reported multiplex analytical assays for nucleic acids, including nanotechnology-based methods and multiplex PCR assays, have been limited to a low number of targets. However, our mμLAMP setup could be easily expanded

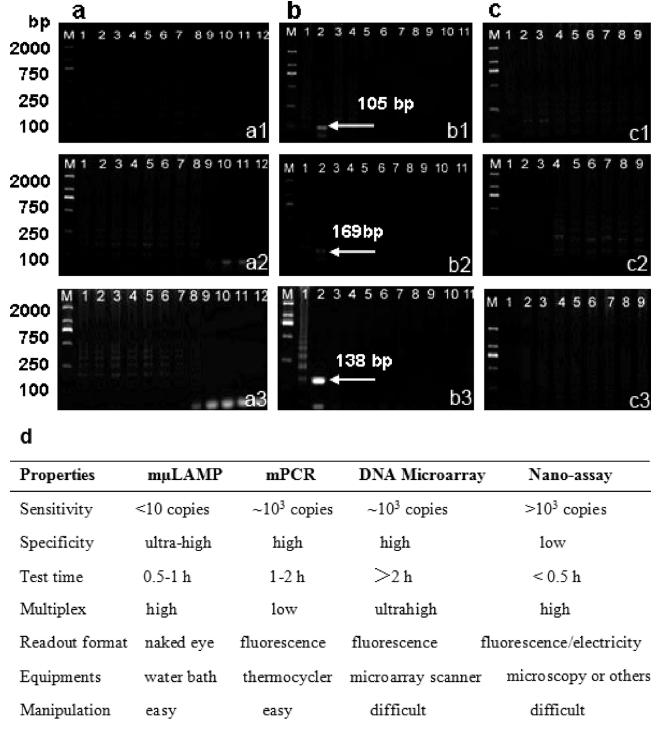


**Figure 4.** Merits of mμLAMP assay. (a) Sensitivity evaluation using 10-fold serial dilutions of standards: a1–a3, sensitivity of the system for flu A virus (a1, lane 1–12,  $8.7 \times 10^7$ ,  $8.7 \times 10^6$ , ...,  $8.7 \times 10^0$ ,  $8.7 \times 10^{-1}$ ,  $8.7 \times 10^{-2}$  copies/μL, blank control, and negative control); seasonal H1N1 (a2, lane 1–12,  $9.7 \times 10^7$ ,  $9.7 \times 10^6$ , ...,  $9.7 \times 10^0$ ,  $9.7 \times 10^{-1}$ ,  $9.7 \times 10^{-2}$  copies/μL, blank control, and negative control); and pandemic H1N1 (a3, lane 1–12,  $7.5 \times 10^7$ ,  $7.5 \times 10^6$ , ...,  $7.5 \times 10^0$ ,  $7.5 \times 10^{-1}$  copies/μL,  $7.5 \times 10^{-2}$  copies/all, blank control, and negative control), respectively. (b) Specificity of the mμLAMP: b1, 1–4, flu A standard, *Pst*I digestion, seasonal H1N1, and pandemic H1N1; b2, 1–4, seasonal H1N1, *Pst*I enzyme digestion, flu A, and pandemic H1N1; b3, 1–4, pandemic H1N1, *Bsm* AI enzyme digestion product, flu A, and seasonal H1N1, respectively. M refers to the DNA marker while 5–11 denotes FMDV, PRRSV, CFSV, TGEV, PRV, negative plasmid control, and blank control, respectively. (c) Response time of mμLAMP for the detection of flu A virus (c1), seasonal H1N1 (c2), and pandemic H1N1 (c3). Lanes 1–9 are 5, 10, 15, 20, 25, 30, 40, 50, and 60 min. (d) Merits of mμLAMP compared to other multiplex assays.

to integrate as many microchambers as possible, thus provide the possibility of analyzing a great number of genes in one system. Apart from differentiating human influenza A virus, we also successfully performed a rapid analysis of eight important swine disease viruses simultaneously in one system with great efficiency and flexibility using this octopus-like mμLAMP device (Supporting Information, Figure S4). Further more, this assay could be applied to, for example, identifying single nucleotide polymorphism (SNP), screening genetic disease-associated genes, analyzing species relationships, and detecting genetically modified organisms/novel artificial lives. The merits of mμLAMP are listed and compared with other typical methods in Figure 4d. Because the system is simple to fabricate/operate, has isothermal analyzing merit, provides a user-friendly readout format, and has a powerful ability to analyze multiple targets qualitatively and quantitatively with high sensitivity and specificity, we think that this technique holds much more significance than the typical DNA microarray and multiplex PCR technique.

in developing point-of-care diagnostic assays to combat various epidemics or genetic diseases, especially in some resource-limited countries.

## METHODS

**Materials.** Conserved nucleic acid fragments of influenza A virus (flu A), seasonal influenza A H1N1 virus (seasonal H1N1), and 2009 pandemic influenza A H1N1 virus (pandemic H1N1) were screened and cloned into the PUC57 plasmid. Plasmids containing the target nucleic acid fragment were used as the standards. The reference strains of flu A, seasonal H1N1, and pandemic H1N1 were prepared in our lab. Swine H1N1, H2N3 virus, classical swine fever virus (CSFV), foot-and-mouth disease virus (FMDV), transmissible gastroenteritis of swine virus (TGEV), porcine reproductive and respiratory syndrome virus (PRRSV), pseudorabies virus (PRV), porcine parvovirus (PPV), porcine circovirus (PCV), and swine influenza virus (SIV) derived from cell culture were provided by the Shanghai Entry-Exit Inspection and Quarantine Bureau. A total of eight clinical throat swab specimens collected from different hospitals during the outbreak of pandemic influenza A (H1N1) virus in 2009 were purchased from the Shanghai Public Health Clinical Center. Total genomic DNAs/RNAs were extracted from the cell culture/throat swab using a QIAamp DNA Blood Mini Kit (Qiagen GmbH, Germany) or Trizol Kit (Invitrogen). Operation of these active viruses was performed in a P2/P3 lab because of the potential biohazard concern. The DNAs/RNAs of the viruses would not cause biohazard problems and could be used in common laboratories.

**LAMPs Establishment.** LAMP was carried out in the system containing 1× ThermoPol Buffer (20 mM Tris-HCl, 10 mM KCl, 10 mM  $(\text{NH}_4)_2\text{SO}_4$ , 0.1% Triton X-100, pH 8.8 at 25 °C), 8.0 mM MgSO<sub>4</sub>, 0.4 mM dNTPs, 0.2 μM each of the outer primer (F3 and B3), 2 μM each of inner primer (FIP and BIP) and 0.8 μM each of the loop primer (LF and LB), 0.2 U/μL of AMV transcriptase, and 0.32 U/μL of *Bst* polymerase with a small amount of sample. Amplification was performed at 63 °C in a water bath for 1 h followed by agarose gel electrophoresis. The final result was directly determined by the naked eye based on the appearance of the white precipitate of magnesium pyrophosphate and the green fluorescence induced by the intercalating dye SYBR green I. An initial experiment was performed to obtain the most optimized LAMP reaction conditions.

**Multiplex LAMP Chip Fabrication and Manipulation.** The master of chip with desired patterns was fabricated by mechanical microfabrication. A PDMS replica was produced by molding as described previously.<sup>22,26</sup> In brief, the PDMS precursor mixture was prepared at a weight ratio of base to curing agent of 10:1 and poured carefully on the master, vacuumed for 0.5 h to get rid of the bubbles, and cured at 80 °C for 2 h. The cured PDMS replica was gently peeled off the master and irreversibly sealed with a microscope glass slide using air plasma to form a leak-proof integral chip. The whole chip was then heated at 121 °C for 30 min to get rid of any contaminants. The 0.6 μL different solutions, each of which contains a specific LAMP probe set (quantities of the probe F3/B3, 1 pmol; FIP/BIP, 10 pmol; LF/LB, 4 pmol) were injected into corresponding microchannels via the end outlet and then evaporated completely, leaving the probes in the microchamber. The whole chip was again treated by the air plasma to obtain a hydrophilic surface of the microchamber.

The 4 μL sample and 46 μL LAMP reaction buffer were sequentially introduced into the system via the center hole by a pipet. The reaction reagent filled all 10 LAMP microchambers symmetrically by capillary force. The inlet/outlet was then tightly sealed with the uncured PDMS to form an integral device. The whole chip was incubated at 63 °C for 1 h using a water bath and the final results were determined using the naked eye or analyzed by agarose gel electrophoresis.

The quantitative *m*μLAMP chip was created by integration with an optical detection unit and a mirror placed under the PDMS replica. The optical unit included reflected optical fibers (FU-65X, Keyence Corporation, Osaka, Japan) and a digital fiber optic sensor (FS-V31M, Keyence Corporation, Osaka), which was used to monitor the real-time changes of the LAMP signal and record the time-to-positive value. (The time-to-positive value, TTP, could be defined as the reaction time necessary for samples to sufficiently reach positive signals above the baseline during real-time amplification.)

The fiber optic sensor employs a high-intensity red (640 nm) light-emitting diode (LED) and a phototransistor. The reflected optical fiber with a 200 μm diameter core and 820 μm diameter cladding was vertically fixed upon the reaction chamber. The mirror underneath the replica was applied to reflect the emission light from the fiber. The decrease of optical density was used to indicate the signal generation by the LAMP reaction and calculated as follows: optical density =  $\ln(I_0/I_1)$  = turbidity, where  $I_0$  is the intensity of incident light and  $I_1$  is the intensity of reflected light.

**System Evaluation and Validation with Various Influenza a Subtypes.** We applied standard samples to evaluate the sensitivity, specificity, and speeding of the *m*μLAMP. The theoretical sensitivity of the system was mainly tested by 10-fold serial dilutions of standards with concentrations ranging from  $10^7$ – $10^0$  copies/μL. The sensitivity of the system for the pandemic H1N1 virus was further compared with standard PCR. To confirm the specificity of the assay, we applied the blank PUC57 plasmid and other nontarget viruses, including FMDV, CSFV, PRRSV, TGEV, and PRV. In addition, we used restriction enzymes *Pst* I to evaluate the reaction product of flu A-probes and seasonal-H1N1 probes and *Bsm* AI for the product of pandemic-H1N1 probes. The rapidity of the system was evaluated by incubating the chip at 63 °C for different times (5 min, 10 min...60 min) and analyzed by gel electrophoresis. In addition to the standard sample, we also used reference samples of flu A, seasonal H1N1, pandemic H1N1, swine H1N1/H2N3, and eight clinical samples to validate our novel developed bioassay.

## ASSOCIATED CONTENT

**S Supporting Information.** Additional information as noted in text. This material is available free of charge via the Internet at <http://pubs.acs.org>.

## AUTHOR INFORMATION

### Corresponding Author

\*E-mail: jlkong@fudan.edu.cn (J.K.); xingyujiang@nanoctr.cn (X.J.).

## ACKNOWLEDGMENT

We are grateful for the kind help from the colleagues in our group and professor Xingyu Jiang's group from the National Center of Nanoscience and Technology for their helpful advice.

We would like to acknowledge the Chinese Academy of Sciences (Grant KJCX2-YW-M15), the Ministry of Science & Technology (Grants 2009ZX10004-505, 2007CB714502, 2009CB930001, 2009ZX10605, and 2011CB933201), the National Science Foundation of China (Grants 20945001, 20890020, 20890022, and 90813032) and Shanghai Leading Academic Discipline Project (Grants B109 and 08XD14010) for financial support.

## ■ REFERENCES

- (1) Ksiazek, T. G.; Erdman, D.; Goldsmith, C. S. *J. N. Engl. J. Med.* **2003**, *348*, 1953–1966.
- (2) Ferguson, N. M.; Cummings, D.; Cauchemez, S.; Fraser, C.; Riley, S.; Meeyai, A.; Iamsirithaworn, S.; Burke, D. S. *Nature* **2005**, *437*, 209–214.
- (3) Smith, G.; Vijaykrishna, D.; Bahl, J.; Lycett, S. J.; Worobey, M.; Pybus, O. G.; Ma, S. K.; Cheung, C. L.; Raghwan, J.; Bhatt, S.; Peiris, J.; Guan, Y.; Rambaut, A. *Nature* **2009**, *459*, 1107–1122.
- (4) Dawood, F. S.; Jain, S.; Finelli, L.; Shaw, M. W.; Lindstrom, S.; Garten, R. J.; Gubareva, L. V.; Xu, X. Y.; Bridges, C. B.; Uyeki, T. M. *N. Engl. J. Med.* **2009**, *360*, 2605–2615.
- (5) Dunbar, S. A. *Clin. Chim. Acta* **2006**, *363*, 71–82.
- (6) Waters, L. C.; Jacobson, S. C.; Kroutchinina, N.; Khandurina, J.; Foote, R. S.; Ramsey, J. M. *Anal. Chem.* **1998**, *70*, 158–162.
- (7) James, D.; Schmidt, A. M.; Wall, E.; Green, M.; Masri, S. *J. Agric. Food Chem.* **2003**, *51*, 5829–5834.
- (8) Schena, M.; Shalon, D.; Davis, R. W.; Brown, P. O. *Science* **1995**, *270*, 467–470.
- (9) Clack, N. G.; Salaita, K.; Groves, J. T. *Nat. Biotechnol.* **2008**, *26*, 825–830.
- (10) Shi, L. M.; Campbell, G.; Jones, W. D. *Nat. Biotechnol.* **2010**, *28*, 109–827.
- (11) Li, Y. G.; Cu, Y.; Luo, D. *Nat. Biotechnol.* **2005**, *23*, 885–889.
- (12) Sha, M. Y.; Walton, I. D.; Norton, S. M.; Taylor, M.; Yamanaka, M.; Natan, M. J.; Xu, C. J.; Drmanac, S.; Huang, S.; Borcherding, A.; Drmanac, R.; Penn, S. G. *Anal. Bioanal. Chem.* **2006**, *384*, 658–666.
- (13) Zhang, C. Y.; Hu, J. *Anal. Chem.* **2010**, *82*, 1921–1927.
- (14) Han, J.; Swan, D. C.; Smith, S. J.; Lum, S. H.; Seferis, S. E.; Unger, E. R.; Tang, Y. W. *J. Clin. Microbiol.* **2006**, *44*, 4157–4162.
- (15) Notomi, T.; Okayama, H.; Masubuchi, H.; Yonekawa, T.; Watanabe, K.; Amino, N.; Hase, T. *Nucleic Acids Res.* **2000**, *28*, e63.
- (16) Mori, Y.; Notomi, T. *J. Infect. Chemother.* **2009**, *15*, 62–69.
- (17) Jiang, X. Y.; Ng, J.; Stroock, A. D.; Dertinger, S.; Whitesides, G. M. *J. Am. Chem. Soc.* **2003**, *125*, 5294–5295.
- (18) Yager, P.; Edwards, T.; Fu, E.; Helton, K.; Nelson, K.; Tam, M. R.; Weigl, B. H. *Nature* **2006**, *442*, 412–418.
- (19) Whitesides, G. M. *Nature* **2006**, *442*, 368–373.
- (20) Ludwig, J. A.; Weinstein, J. N. *Nat. Rev. Cancer* **2005**, *5*, 845–856.
- (21) Mori, Y.; Nagamine, K.; Tomita, N.; Notomi, T. *Biochem. Biophys. Res. Commun.* **2001**, *289*, 150–154.
- (22) Fang, X. E.; Liu, Y. Y.; Kong, J. L.; Jiang, X. Y. *Anal. Chem.* **2010**, *82*, 3002–3006.
- (23) Chen, Q.; Li, J.; Fang, X. E.; Xiong, W. *Intervirology* **2009**, *52*, 86–91.
- (24) Beer, N. R.; Wheeler, E. K.; Houghton, L. L.; Watkins, N.; Nasarabadi, S.; Hebert, N.; Leung, P.; Arnold, D. W.; Bailey, C. G.; Colston, B. W. *Anal. Chem.* **2008**, *80*, 1854–1858.
- (25) Visconti, M. R.; Pennington, J.; Garner, S. F.; Allain, J. P.; Williamson, L. M. *Blood* **2004**, *103*, 1137–1139.
- (26) Qin, D.; Xia, Y. N.; Whitesides, G. M. *Nat. Protoc.* **2010**, *5*, 491–502.